Catalytic reforming of tar and volatiles from walnut shell pyrolysis over a novel Ni/olivine/La$_2$O$_3$ supported on ZrO$_2$

Babalola Aisosa Oni [a,b,*], Samuel Eshorame Sanni [b], Sunday Olayinka Oyedepo [c], Anayo Jerome Ibegbu [d]

[a] Department of Chemical Engineering, China University of Petroleum, Changping District, Beijing City, PR China
[b] Department of Chemical Engineering, Covenant University, Ota, Nigeria
[c] Department of Mechanical Engineering, Covenant University, Ota, Nigeria
[d] Department of Mechanical Engineering, Madonna University, Enugu, Nigeria

ARTICLE INFO

ABSTRACT

The effect of catalytic reforming of volatiles from pyrolysis of walnut shell using an innovative catalyst was investigated in this study. The analysis was conducted in a two-stage fixed bed reactor operated at 700–1100 °C. The prepared Ni/olivine/La$_2$O$_3$/ZrO$_2$ catalyst had a significant performance on the catalytic tar reforming reactions. In the catalytic reforming of tar, the weight of catalyst is critical. However, it was observed that the tar reforming efficiency increased with increase in catalyst-weight and temperature. In addition, the highest tar reforming efficiency (98.9%) was attained with 20 g of Ni/olivine/La$_2$O$_3$/ZrO$_2$. After 4 cycles of regeneration, tar reforming efficiency was kept stable. The product gas composition was highest at 1100 °C with a very low tar yield, which reduced from 18.1 to 2.1 wt% at 700–1100 °C. At varying reforming conditions, the product gas composition increased. The product-gas distribution varied at different steam flow rates (3–9 mL/h) as well as particle size (0.2–3.5 mm) and the highest yield was achieved with the smallest particle size (0.2 mm) of walnut shell thus confirming the superb catalytic activity of Ni/olivine/La$_2$O$_3$/ZrO$_2$ for tar reformation into gases owing to high dispersion of ZrO$_2$ in the shells.

1. Introduction

Gasification or pyrolysis of biomass is a promising technology for global sustainable energy systems because of its potential to curb the overreliance on conventional fuels [1]. Using a thermochemical conversion process, the technology converts biomass into combustible gas in a clean and efficient manner [2]. The combustible pyro-gas can be used for the production of power in most equipment in the industries from steam cycles through gas engines and turbines. Clean pyro-gas can be used as a gas fuel due to its high low heating value [3,4]. It can also be used as a make-up heat source during the process of pyrolysis. During gasification, the product gas obtained is mainly syngas, which has wide range of applications in the process industries [4]. Syngas can be used making chemical-fuel, gas turbine fuel, the anode gas of solid oxide fuel cells, and as raw material for synthetic natural gas, renewable energy fuels, fertilizers and liquid fuels. The produced hydrogen from biomass gasification can be used as transportation fuels as well as for electric power generation [5].

Many parameters including heating rate, reaction temperature, and material qualities, influence the yield and distribution of products during biomass pyrolysis [2,3]. Nevertheless, gasification or pyrolysis of biomass produces gaseous products as well as undesirable by products such as tar [3], which remains a barrier to widespread adoption of this technology; additionally, steam-reforming is efficient in enhancing the formation of gaseous products thus reducing the tar content while increasing the rate of thermal conversion of biomass to gaseous products [1,4,5].

Tar from biomass catalytic reforming processes is a complex mixture of non-condensable and condensable hydrocarbons, which range from single to 5- ring aromatic molecules, as well as various oxygenated and polycyclic aromatic hydrocarbons (PAHs) [6]. Aromatic chemicals such as C$_6$H$_6$ and PAHs in tar, are poisonous and can pollute the environment [3]. Tar can build up on the surface of the bed of catalyst within the reactor alongside heat exchangers and filters.

There are three types of tar removal technologies, they include chemical, biological, and physical technologies. In biological

---

technology, the active biological enzyme in the microorganism may successfully remove tar components [7]. The electrostatic force, inertia collision, gravity, interception, and diffusion methods are used for tar removal from the gaseous phase into the liquid phase [1,8]. Partial oxidation, thermal cracking, and other chemical methods are used to transform the tar component into gases (CH_4, CO, CO_2, and H_2).

Tar, as a major problem and barrier in gasification process, has a number of negative consequences for rapid development and widespread application, including the following: (a) it can block devices and pipelines at a low temperature that is below dew point (about 300 °C) [8]. The gaseous tar in the carrier gas will quickly condense, after which it subsequently combines with water and other particles that can easily stick to the cleaning equipment/gas pipeline, and eventually block the system [1,5]. (b) Tar-acidic components have the potential to cause significant corrosion in downstream pipelines and devices. Furthermore, when tar-containing fuel gas is burned in an engine, it produces high-temperature soot and smoke, thus corroding the gas nozzle which in turn affects the entire combustion system [4,9]. (c) When a catalyst is deactivated at a high temperature, the carbon/soot produced deposits on the catalytic surface, thus inactivating the active site and reducing the catalyst's service life [2,6]. (d) Tar reduces the efficiency of gasification and (f) degrades the plant's production environment [1]. Many of the benzene-based chemicals found in tar are cancerous. This will not only endanger the health of workers at the gasification plant, but it will also pollute the environment when released [4].

Catalytic reforming, physical elimination, and thermal cracking, are some of the methods for eliminating tar. However, catalytic reforming is a potential method for optimizing tar conversion to product gas of high quality in the presence/absence of steam during biomass pyrolysis [2,5, 8]. The volatiles received from biomass gasification or pyrolysis, can be routed through a reforming catalyst, where large molecules of tar can be broken into a range of tiny gaseous molecules, predominantly combustible gaseous components such as hydrogen and carbon(II)oxide to obtain tar-free product gas [9].

The catalytic reformation of tar at temperatures between 600 and 900 °C has been extensively researched [6]. According to other authors, nickel, and some transition metals supported on ceramic and alumina as well as, olivine, noble metals, and dolomite have all demonstrated high tar reforming activities [3,5,9–12]. Catalysts such as Rhodium, Ruthenium, and Platinum have also proven to be very efficient for tar reforming, however, despite being very expensive, they are usually unsuitable for reforming processes, hence the need for the use of nickel-based catalysts [11]. Low loadings (0.5 wt percent) of such noble metals such as Mg–Ce–Zr–O mixed-metal oxides, were evaluated for their cost reduction potentials during reforming reactions [12]. The catalysts showed high catalytic activities at low temperatures thus confirming their reliabilities in stimulating tar reforming reactions. At low temperatures, Ni-based catalysts have been found active in tar reforming processes [8–13]. Olivine, char, and dolomite seem to be particularly appealing among these supports, as they are all very affordable and readily available [7,11]. Although olivine is less efficient in gasification processes, it has the ideal hardness required for application in fluidized-bed reactors. Also, because the catalytic activities of olivine and dolomite for tar conversion can be improved, the objective is to induce high catalyst selectivity as well as catalyst-supports and promoters [5,9].

One of the most important aspects of improving catalyst activity and stability is choosing the right support/promoter. According to Santamaria et al. [14], La_2O_3 is a good support for nickel catalyst because it provides high stability and performance with improved conversion and hydrogen yield of about 91% and hence, the integration of metal oxide promoters may significantly improve both the stability and performance of the catalyst. As a result, a good promoter can improve the following characteristics: i) mechanical properties which include high resistance to attrition and mechanical strength, which is critical in fluidized bed reactors; ii) physical characteristics, which facilitate better nickel

dispersion thus impeding deactivation by metal sintering while improving the accessibility of bio-oil molecules thus, preventing porous structure blockage; iii) reducibility of metallic species, which require less nickel active phases on the catalysts with faster catalyst-deactivation [4,10,11,13,15]. Nonetheless, due to catalyst deactivation, biomass conversion and H_2 production declined dramatically with time on-stream. In order to optimize H_2 production and catalyst stability, a wide range of catalyst supports have been discussed [4,15]. Thus, steam reforming reactions of volatiles produced from biomass pyrolysis have been extensively investigated using common metal oxide supports (Al_2O_3, MgO, SiO_2, TiO_2, or CeO_2). Furthermore, due to their reduced costs, other supports such as ZrO_2 are gaining attention. Yang et al. [16] studied hydrogen production in catalytic reforming of pyrolyzed corncob volatiles using Nickel, Cobalt, and Nickel–Cobalt catalysts promoted with acid washed lignite, with the bimetallic catalyst producing the highest amount of hydrogen. In the pyrolytic-gasification of biomass, Ye et al. [17] achieved a hydrogen generation of 4.2 wt% via a nickel catalyst supported on MCM-41. Thus, the ZrO_2 support was seen to display outstanding characteristics, including: (i) an amphoteric character as a result of the basic and acid properties on its surface, which impact redox functions on the support [2,12], ii) high thermal stability and mechanical strength, and iii) the potential to enhance steam adsorption and thus activating the gasification of HCs adsorbed on the surface of the catalyst in steam reforming reactions, which contribute to increasing the amount of recovered hydrogen [15,18]. The structure of ZrO_2 as well as the type of phases generated during its production process, has a major impact on the performance of the nickel/olivine/La_2O_3/ZrO_2 catalyst. As a result, the tetragonal phase of ZrO_2 has been determined to be the most suitable geometry for application. Despite the fact that several nickel-promoted catalysts have been studied and developed for steam reforming of oxygenates, no information about the performance of the Ni/olivine/-La_2O_3/ZrO_2 catalyst in the two-step process of biomass pyrolysis and in-line steam reforming of volatiles has been found in literature. In order to improve the catalytic performance and stability of Ni/olivine/-La_2O_3/ZrO_2 in biomass pyrolysis, this study then focuses on investigating and enhancing the impact of Ni/Olivine catalyst with La_2O_3 and ZrO_2 in biomass pyrolysis with the aim of converting or reforming tar to form more syngas.

2. Materials and method

2.1. Biomass properties

Walnut shells were collected from Ota, South-West Nigeria. The collected walnut shells were washed with tap water and distilled water to remove dirt and sand particles. The shells were later sun dried for 24 h and subsequently dried in an oven at 105 °C. The dried biomass was crushed to a particle size of 0.05–2 mm. Ultimate and proximate analyses were carried out on the shells using the Vario MICRO Cube

Table 1
Proximate and ultimate analysis of Walnut shell biomass.

Proximate analysis (wt. %)[a]	
Fixed carbon	24.38[c]
Moisture	0.01[a]
Volatile matter	74.19[c]
Ash	1.42[c]
Ultimate analysis (wt.%)	
Hydrogen	5.74[b]
Oxygen	43.99[b]
Carbon	50.02[b]
Nitrogen	0.25[b]

[a] Wet basis.
[b] Dry ash-free basis.
[c] Dry basis.

analyzer, Elementa, France; the results are as presented in Table 1.

2.2. Ultimate and proximate analyses of walnut shells

Table 1 shows the proximate and ultimate analysis of the walnut shell biomass, which has a fixed carbon of 24.38 wt% and has a high carbon content of 50.02 wt % which makes it a suitable biomass for catalytic reforming of tar over the novel catalyst.

2.3. Catalysts

2.3.1. Synthesis of the catalyst

A 20 wt% Nickel was first synthesized using the method of wet impregnation with the precursor $Ni(NO_3)_2 \cdot 6H_2O$ (VWR Chemicals, 99%) dissolved in deionized water and heated to 110 °C until a precipitate of nickel was formed. 20 g of olivine was added to the nickel. The resulting mixture was maintained in the ratio 1:1, and further calcined in a muffle furnace at 1250 °C for $2\frac{1}{2}$ h under atmospheric condition. The obtained catalyst was ground and sieved to obtain different particle sizes.

To enforce nickel loading, the prepared Ni/olivine admix was promoted with (La_2O_3) by mixing in ratio (2:1); the La_2O_3 was obtained via sol-gel technique from micro-sized La_2O_3 powders, high-molecular weight polyethylene glycol (PEG) and 20% nitric acid as precursors. The metal promoter oxide concentration was fixed at 20 wt% La_2O_3. A portion of ZrO_2 (meant to serve as catalyst-support) was pre-treated in order to attain suitable fluidization in the reforming step and was thereafter, dried for 24 h at 110 °C and calcined at 1200 °C for $2\frac{1}{2}$ h. A 20 wt% of (ZrO_2) was used. The support was sieved and ground to 0.4 and 0.8 mm particle size. After the preparation of the catalyst-support, it was later admixed with Ni/olivine/La_2O_3 in the ratio of 1:1. The catalysts obtained were sealed in a bag and stored in a desiccator.

Note: Several other proportions of mixing ratios of the catalyst were adopted during experimentation for optimal catalytic reforming of tar and volatiles for walnut shell pyrolysis.

2.4. Estimation of tar-conversion efficiency

The catalytic cracking/conversion of tar can be estimated using equation (1).

$$\eta_{tar} = \frac{X_{yd} - X_{yr}}{X_{yd}} \times 100 \% \qquad [1]$$

The tar conversion efficiency (TCE) can be expressed as η_{tar}, while X_{yd} and X_{yr} represent biomass tar yield before and after reforming, g/g.

2.4.1. Experimental procedure

A two-stage quartz fixed-bed reactor was used to catalytically reform the biomass into volatiles. The process involves heating the biomass to generate tar which was later reformed using Ni/olivine/La_2O_3/ZrO_2 catalyst. The reactor comprises of quartz filled to a length of 840 mm and an inner diameter of 285 mm (Fig. 1). The catalyst bed was approximately 30 mm away from the steam supply inlet.

The fixed-bed was divided into two sections (lower and upper), its top and bottom segments have lengths of 400 mm and 540 mm, respectively which were electrically heated with two thermocouples using a 2 -zone electrical heater/furnace (220 ∼ 240 V) with a power rating of 2.0 kW. The heater/furnace maintained the heating process of the reactor over 190 mm length in each zone. The feeding of biomass into the reactor commenced when the reactor temperature was uniform (700 °C); 100 g of walnut shell (biomass) was loaded in the feeder at 100 mg/min. The bed material is made up of silica-sand with size range of 212–300 μm. The catalyst (20 g) was pre-loaded in the reactor's lower stage, where the height of the loaded catalyst bed lies within 23 ∼ 25 *mm*. The slight variation in the catalyst loading height controls the reaction time for the catalysts during the tar reforming process. 99.8% pure N_2 was used as the carrier gas which flowed at the rate of 80 mL per minute to keep the reactor-interior inert while receiving the gaseous products.

The upper segment of the 2- stage fixed bed layer was set at 700 °C, while the lower stage was maintained at 700–1000 °C to monitor the tar reforming process over the Ni/olivine/La_2O_3/ZrO_2 catalyst. The duration of each experiment was 15 min which helped to ensure that the reaction was complete prior tar reforming.

For the experiments involving steam reforming, the steam was fed via a pump for 10 min from the commencement of the reforming process. With the use of a High-performance liquid chromatographic (HPLC) pump, steam was produced from water that was delivered directly into the reactor (Alltech 426). The steam entered the reactor mid-way between the two stages. Control experiments were conducted
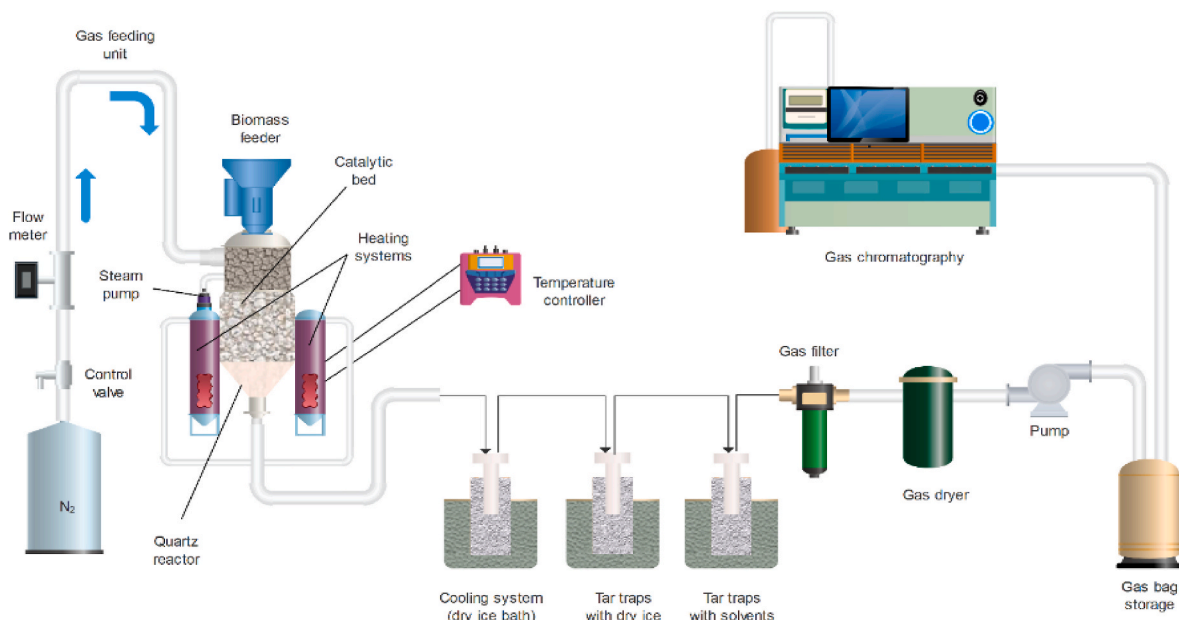

Fig. 1. Schematic representation of reforming of volatiles from walnut shell.

at the same conditions without the use of catalyst. The reactor was cooled to 27 °C under nitrogen atmosphere at the end of each run of the experiment.

The produced gas/syngas (hydrogen, methane, carbon dioxide, carbon monoxide, and light hydrocarbons (C_2H_4, C_2H_6) flowed out of the fixed-bed reactor and passed through an ice water trapping unit and later through a solvent (pure chloroform) unit which helped to cool and absorb the tar respectively. The product gases were filtered and dried and then pumped into a gas bag for storage.

Thus, the volume concentrations of the four components (H_2, CH_4, CO, CO_2) in the sampled gas were further analyzed using the Agilent 7880 gas chromatography (GC) which is fitted with thermal conductivity detector (TCD). The experiment was carried out in triplicates to validate the experiment's reproducibility, and the mean data were used to obtain the final results.

Quantitative calibration was conducted using standard gas mixtures, during the process of analysis using helium as the carrier gas. Furthermore, at about 65 °C, the tar-pure chloroform solution was heated using a rotary evaporator for the removal of the pure chloroform, and the obtained residue was weighted as the tar yield. Blank experiments in the absence of char catalysts were also carried out for the purpose of comparison.

3. Results and discussion

3.1. Catalyst characterization

3.1.1. Pore size distribution of the catalyst

The pore size distributions of raw Ni/olivine/La_2O_3/ZrO_2 and thermally treated Ni/olivine/La_2O_3/ZrO_2 are presented in Fig. 2. The peak occurrence at 2.8 nm for the raw Ni/olivine/La_2O_3/ZrO_2 is as a result of the micropores from the interparticle clearance. After heating at 800 and 900 °C, a robust peak occurred above 1.2 nm. When heated to 1000 °C, the peak moved to 3.5 nm, and the intensity decreased as the temperature increased. The increase in specific surface area of the catalyst is as a result of the slit-shaped micropores. The micropore in the Ni/olivine/La_2O_3/ZrO_2 disappeared at 1100 °C. The uniform mesopores at 4.5 nm, provide an exceptional atmosphere for the reforming of volatiles. Thus, with an increase in temperature, the micropores that were newly formed were transformed into macro-pores and mesopores, due to an increase in pore size and a decrease in specific surface area. The Brunauer-Emmett-Teller (BET) analysis shows the total pore volume, BET surface area and average pore size of biomass/catalyst ratio (100 g/20 g) with optimum
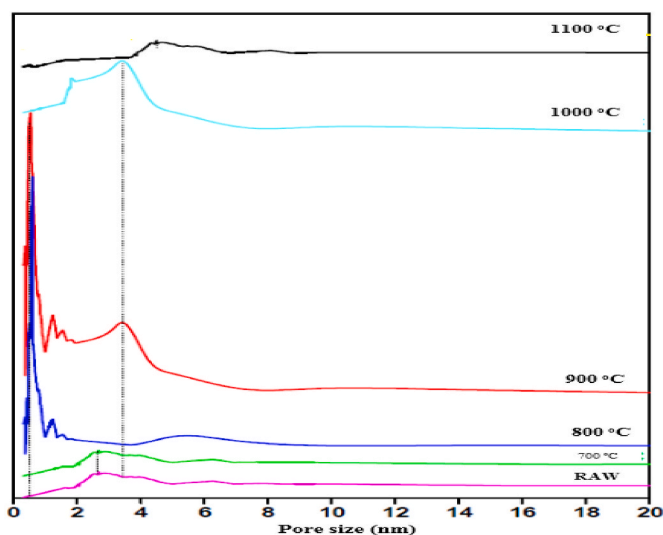
performance at temperatures of 700, 800, 900, 1000, 1100 and 1200 °C. At 1100 °C, the catalyst performed optimally with respect to the fixed biomass/catalyst ratio. The biomass/catalyst ratio (100 g/20 g) performed best, thus, further heating at a higher temperature (1200 °C) reduces the catalyst performance. From Table 2, the biomass/catalyst ratio (100 g/20 g) @ 1100 °C, gave the highest surface area, total pore volume and average pore size of 335.72 cm^3/g, 0.58 cm^3/g and 0.30 nm respectively compared to others. A further increase in the biomass/catalyst ratio reduces the surface area, total pore volume as well as the average pore size which also affects the tar conversion efficiency.

3.1.2. Scanning electron microscopy (SEM)

SEM model FE-II-QUAT 2000 was used to examine the best catalyst's surface at different temperatures (700–1200 °C). The catalyst surface morphology-conjugates as well as the catalyst pore structure available for adsorption were revealed by SEM (Fig. 3a and b). The catalyst was studied under optimal circumstances using argon gas at atmospheric pressure. As shown in Fig. 3a, the fresh unheated catalyst is seen to contain the narrowest pores which was also confirmed by the BET results given in Table 2. In Fig. 3b, the pore size of the catalyst increased owing to the fact that it was heated at 700 °C. Further increase in temperature, resulted in further expansion or widening of the catalyst's pores which led to an increase in reactant concentration at the active sites of the catalysts, thus resulting in increased interactions between reactant molecules which was induced by the lowering of the activation energy of the reactants; this then implies that the rate of product formation increased at increased temperatures from 700 to 1100 °C (Fig. 3b (B-E)). This trend is also justified by the decreased pore size of the catalyst at increased temperatures (Table 2). However, upon increasing the temperature further to 1200 °C(see Fig. 3b(F)), the rate of gas production reduced which may have been caused by catalyst coking/blockage or pore rupturing that may yield particle agglomeration which then hinders high gas production. Also, issues related to the shielding effects of other accumulated products/un-desorbed products from the pore sites may cause hindering effect, which then prevents further penetration of reactants within the catalyst pores for conversion to products. Hence, the optimum performance or normalized condition for the highest gas production is at 1100 °C. A review of some selected works are presented in Table 3.

3.1.3. The X-ray diffraction patterns (XRD) of the catalyst at different temperatures

The XRD patterns of the fixed biomass/catalyst ratio (100 g/20 g) heated at different temperatures are presented in Fig. 3c. Thermal treatment of the catalyst was conducted from 700 °C–1100 °C; only one low broad diffraction peak was observed at 700 °C, thus suggesting an initial activation of the catalyst. At 700–900 °C, the catalyst, supports and promoter had mixed interactions such that all components contributed almost equally to the catalyst's activity. However, at > 900 °C, high peak intensities of olivine and zirconia became evident which helped to boost the catalyst's activity even up to 1100 °C i.e., high peak intensities of the constituents of the catalyst became evident at 900 °C–1100 °C thus indicating increased catalyst activity at such temperature range. Furthermore, as the temperature increased, nickel

Fig. 2. Pore size distribution of raw Ni/olivine/La_2O_3/ZrO_2 and thermally treated Ni/olivine/La_2O_3/ZrO_2.

Table 2

Total pore volume and surface area of the Ni/olivine/La_2O_3/ZrO_2 catalyst @ 1100 °C optimum condition.

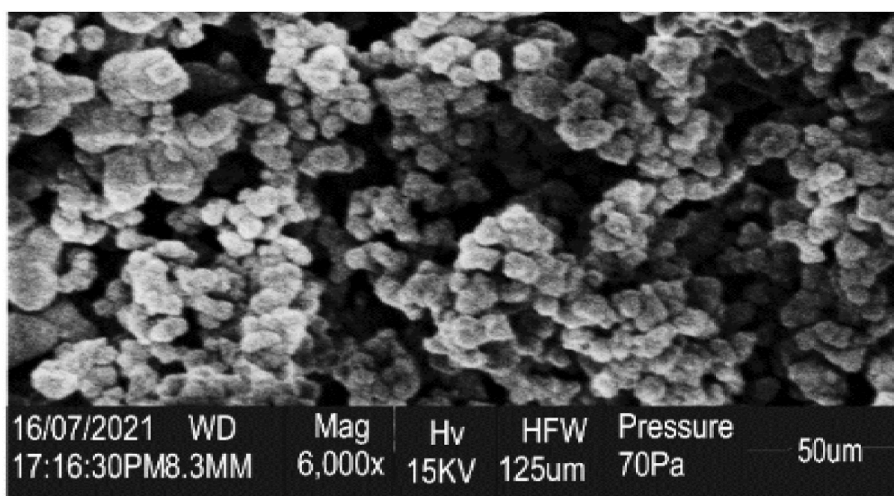| Biomass/catalyst ratio (100 g/20 g)	Total pore volume (cm^3/g)	BET surface area (cm^3/g)	Average Pore size (nm)
700 °C	0.14 ∓ 0.01	200.03 ∓ 3.26	0.07
800 °C	0.21 ∓ 0.09	219.81 ∓ 1.40	0.09
900 °C	0.33 ∓ 0.05	269.97 ∓ 3.09	0.16
1000 °C	0.35 ∓ 0.02	273.54 ∓ 2.08	0.19
1100 °C	0.47 ∓ 0.08	335.72 ∓ 4.46	0.30
1200 °C	0.37 ∓ 0.03	275.72 ∓ 2.94	0.22

Fig. 3a. SEM image of Ni/olivine/La$_2$O$_3$/ZrO$_2$ fresh catalyst without heating.
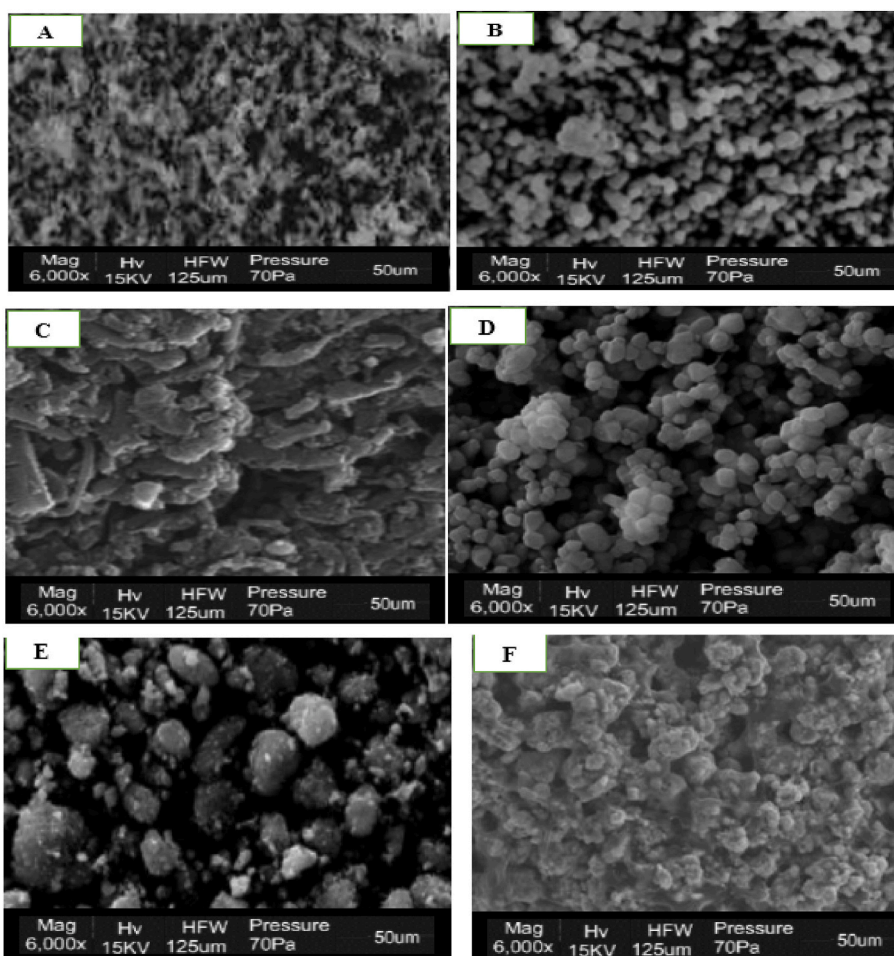

Fig. 3b. SEM Images on catalytic activities at optimal yield of biomass/catalyst ratio (100 g/20 g): Conditions: A(700 °C); B(800 °C); C(900 °C); D(1000 °C); E (1100 °C); F(1200).

sintering was prevented by the comingling of olivine with the promoter (La$_2$O$_3$) and the other catalyst-support (ZrO$_2$), which did not only provide sufficient stability but also restricted any tendency for pore contraction with improved catalyst selectivity. The presence of La$_2$O$_3$ in the catalyst increased the dispersion of the catalyst in the biomass with an improvement in the number of active sites and stability of the catalyst, thus enhancing the resistance to tar formation since the Ni–La$_2$O$_3$ interaction strengthens the catalyst for high catalytic performance. At 1100 °C, the two peaks corresponding to $2\theta = 34.7°$ and $2\theta = 35.9°$ merge into a single broad peak, which is ascribed to the strong diffraction peak of the olivine associated with La$_2$O$_3$, and ZrO$_2$. At $2\theta > 40$, there is a high occurrence of the ZrO$_2$, thus indicating that at

Table 3

Review of some selected works on Catalytic Reforming of Tar and Volatiles.

| Refs.	Catalyst	Biomass used/component	Reforming efficiency
[31]	Ni/MS catalyst (Ni/magnesium slag catalyst)	cellulose, hemicellulose and lignin.	89.4, 92.0, and 94.8% for lignin cellulose, and hemicellulose.
[31]	Ni/MS catalyst (Ni/magnesium slag catalyst)	pine and straw	94.4% and 92.5% for pine and straw
[33]	Natural limonite ore	corncob	83%
[34]	Char-supported catalysts and ilmenite	mallee wood	84% and 96%
[35]	Goethite; specularite; hematite	lignite blended with corn straw	83.9; 84.2 and 87.6%
This study	Ni/olivine/La$_2$O$_3$ supported on ZrO$_2$	Walnut shell	98.9%
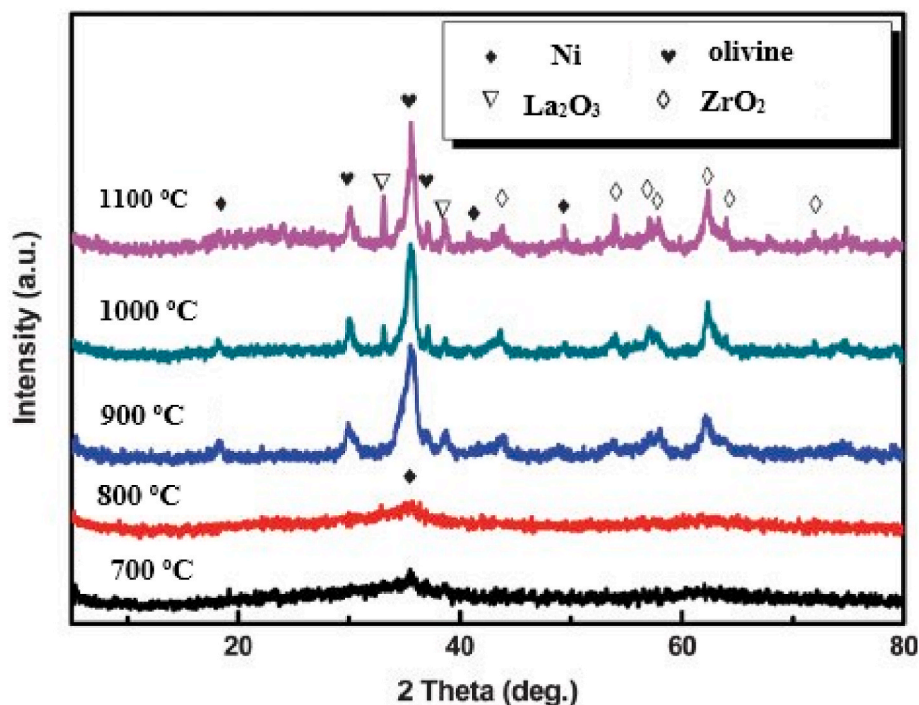
Fig. 3c. XRD patterns of catalyst activity at optimal yield of syngas. Condition: Biomass/catalyst ratio (100 g/20 g).

such condition, the increased interactions of the two supports (olivine and ZrO2) helped to prevent the susceptibility of Ni to sintering, owing to the improved penetration of both compounds in the catalyst to prevent contraction of the Ni pores and thermal degradation of the catalyst.

Considering the new catalyst system reported in this study, the presence of olivine did not only prevent Ni-sintering but also helped to enhance tar conversion to gas, thus lowering any tendencies for catalyst-poisoning by residual tar, which were evident at lower temperatures.
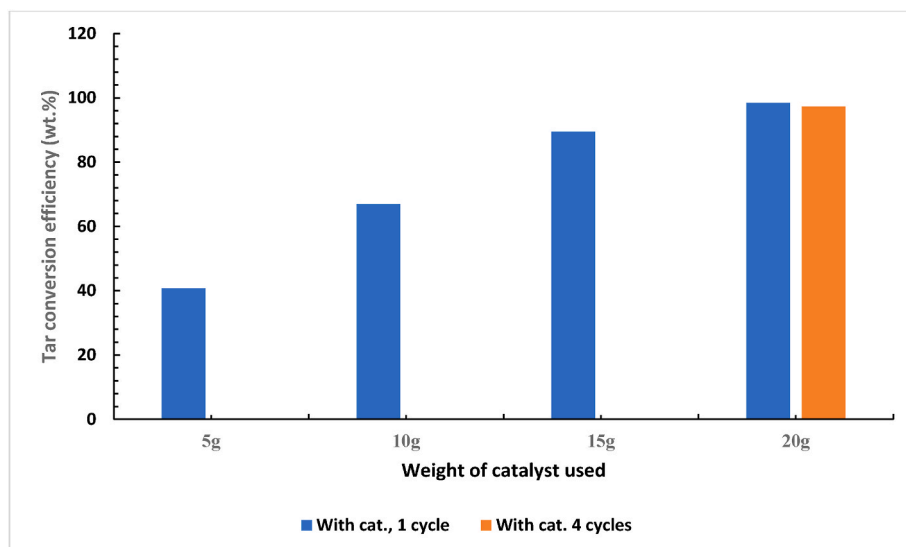

Fig. 4. Effect of catalyst weight on tar reforming.

In addition, the inclusion of ZrO_2 in similar catalyst formation, have been reported to give rise to a unique kind of interaction within the active phase of the catalyst which resulted in tar reforming reactions to yield gaseous products. In essence, the possible synergistic effects of ZrO_2 and olivine undoubtably improved the new catalyst's (Ni/olivine/La_2O_3/ZrO_2) activity.

3.2. Effect of catalyst weight on tar reforming and regeneration

For catalytic reforming of tar, the weight of the catalyst is critical. It is inefficient to utilize an excessive amount of catalyst for tar catalytic reformation. Furthermore, the barrier to gas percolation when flowing through the pores of the catalyst may be enhanced. To put it in another way, if the catalyst is insufficient, the tar reforming efficiency is reduced [18]. Additionally, due to the short retention period, the catalyst is easily deactivated; as a result, an excess catalyst can enhance the frequency and reaction duration of active sites with tar molecules, thus improving the performance of the catalyst. Fig. 4 depicts the effect of biomass/catalyst ratio on tar reforming efficiency at 1000 °C. The efficiency of tar reforming increased as the biomass/catalyst ratio increased. For biomass/catalyst ratio (100 g/5 g), the tar-reforming efficiency was 40.7%. However, upon increasing the biomass to catalyst weight ratio to (100 g/15 g) and (100 g/20 g), the tar-reforming efficiency rose to 89.5 and 98.4%, respectively. These were caused by the increased weight of the catalyst which improved the catalytic reaction and retention time. Addition of more than 100 g/20 g biomass/catalyst ratio did not increase the tar reforming efficiency further, rather, the tar reforming efficiency decreased after 4 cycles, thus suggestive of a high stability and good performance within 4 cycles of tar conversion; these results corroborate the findings of refs. [19–21].

3.3. Catalytic behavior of Ni/olivine/La_2O_3/ZrO_2

Using Ni/olivine/La_2O_3/ZrO_2 as catalyst, the effect of temperature in the range of 700–1100 °C on tar conversion efficiency was studied. Fig. 5 illustrates the tar conversion efficiency with and without catalyst addition. There was an increase in temperature for all cases. The biomass was fixed at 100 g with different weights of catalyst added (i.e., 5, 10, 15 and 20 g) respectively in the reactor. The TCE increased from 23 to 55.0% after increasing the reforming temperature from 700 to 1100 °C without

the addition of catalyst, thus showing the temperature effect on the thermochemical decomposition/reforming of tar. However, with the addition of Ni/olivine/La_2O_3/ZrO_2 as catalyst in different (biomass/catalyst) ratios, there was an increase in TCE up to 98.9% throughout the reforming process between 700 and 1000 °C. This is an indication that the catalyst is very effective in tar conversion and this is in agreement with the findings of refs. [7,11,15–17]. The catalyst with good porous structure not only has good absorbability and large specific surface area, but also imposed speed and reformation owing to the alkaline earth metal and alkaline metal that are attached to its surface. Thus, Ni/olivine/La_2O_3/ZrO_2 can excellently promote tar cracking as a result of its catalytic activity on tar conversion. For a fixed biomass quantity (100 g)/different catalyst weight of 5, 10, 15 and 20 g, the optimal tar conversion efficiencies were 66%, 79%, 85% and 98.9% respectively.

However, further increase in the biomass/catalyst ratio had no effect on the tar reforming process. Therefore, a higher catalyst activity of Ni/olivine/La_2O_3/ZrO_2 for biomass conversion can be obtained using biomass/catalyst ratio (100 g/20 g), thus resulting in higher tar conversion.

The results in Table 3 presents the catalytic reforming of Tar and volatiles of different biomass feedstock from previous works. The Ni/MS catalyst (Ni/magnesium slag catalyst) gave the highest reforming efficiency of 94.8% from cellulose, hemicellulose and lignin biomass, as compared to that obtained in this study (98.9%). The use of corncob, mallee wood, pine and straw and lignite blended with corn straw biomasses gave reforming efficiencies of 83, 96, 94.4 and 87.6% for their respective catalysts (Table 3). However, the use of Ni/olivine/La_2O_3 supported on ZrO_2 with walnut shell marginally improved the tar conversion to 98.9% using walnut shell biomass as compared to other literature (Table 3) in a fixed bed reactor due to the activity of the catalyst.

3.4. Temperature effect on tar yield during catalytic reforming

In Fig. 6, there was an increase in tar yield to 19.9% from 700 to 800 °C, whereas, above 800 °C, the tar yield decreased sharply as a result of high pyrolysis temperature. It can be seen that reforming at 800 °C results in the total release of volatile matter and a substantial tar production, making it possible to monitor tar conversion during the cracking process.
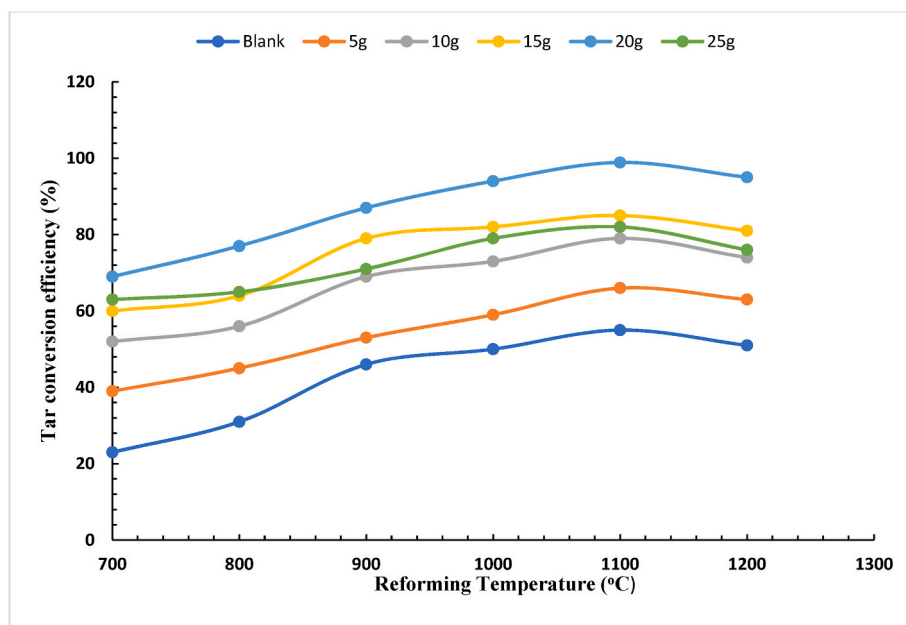

Fig. 5. Effect of reforming temperature on tar conversion efficiency at different catalyst weight.
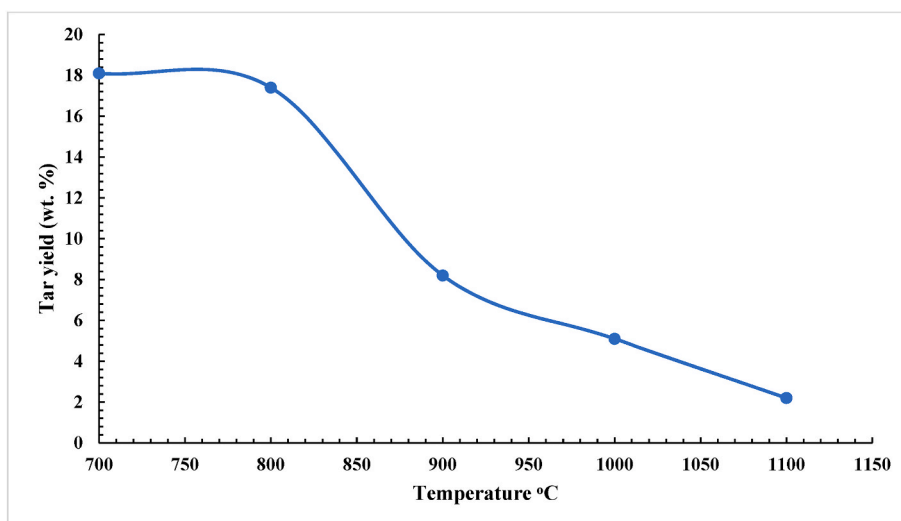
Fig. 6. Temperature effect on Tar yield wt. %.

3.5. The effect of steam flow rate and biomass particle size on tar conversion and yield

Fig. 7a, b, c and d depict the effects of steam flow rate and biomass particle size on tar conversion and yield. Using Ni/olivine/La$_2$O$_3$/ZrO$_2$ as catalyst with steam at a flowrate of 10 mL/h in Fig. 7a, an increase in temperature in the range of 700–1000 °C increased the tar conversion efficiency but tar conversion dropped beyond 1100 °C, which may be due to catalyst deactivation. The biomass was fixed at 100 g with different ratios of catalyst weight added (5, 10, 15 and 20 g) respectively (biomass/catalyst ratio) in the reactor. The tar conversion efficiency increased from 13 to 45.0% after increasing the reforming temperature from 700 to 1100 °C without the addition of catalyst, thus showing the temperature-effect on the thermochemical decomposition/reforming of tar. With the novel catalyst addition/steam (10 mL/h) at different weight percents, there was an increase in TCE up to 88.9% at biomass/catalyst ratio (100 g/20 g), throughout the reforming process between 700 and 1100 °C; for increase in particle size, the TCE was up to 87.3 as shown in Fig. 7c for 20 g weight of catalyst. The catalyst gave high efficiency in the tar reforming process. Thus, Ni/olivine/La$_2$O$_3$/ZrO$_2$ can excellently promote tar cracking as a result of its catalytic activity during tar conversion. Again, further addition or increase in the amount of catalyst on the biomass had no effect on the tar reforming process. Therefore, a higher catalyst activity of Ni/olivine/La$_2$O$_3$/ZrO$_2$ for biomass conversion can be obtained using biomass/catalyst ratio (100 g/20 g), thus resulting in higher tar conversion. In Fig. 7b and d, the tar yield for catalyst/steam decreased from 23.1 to 3.2% when the temperature increased from 700 to 1100 °C (Fig. 7b), whereas, for catalyst/particle size (0.2–0.49 mm) (Fig. 7d), the tar yield decreased sharply from 15.9 to 3.9% as a result of an increase in the pyrolysis temperature from 700 to 1100.

3.6. Composition of syngas under different reforming conditions

Synthetic gas is the main product from biomass gasification and pyrolysis. Fig. 8 a-d display the yield of syngas i.e., hydrogen, carbon monoxide, methane, and carbon dioxide respectively at several reforming conditions and their respective gas compositions. The yield of syngas increased with the addition of Ni/olivine/La$_2$O$_3$/ZrO$_2$ in the biomass which may be due to the high thermochemical reactions in the biomass as stimulated by Ni/olivine/La$_2$O$_3$/ZrO$_2$ as well as other reaction conditions in the reactor. Temperature plays a major role on the gas yield. The possible mechanisms of tar reforming using Ni/olivine/La$_2$O$_3$/ZrO$_2$ catalysts may be expressed by the homogeneous and heterogeneous reactions shown in the supplementary section (S1). The consecutive increase in the yield of syngas with catalyst and temperature addition depends on the gaseous products produced by these reactions [19–21].

The catalyst in walnut shell (biomass) may absorb the tar components, thus resulting in the complete elimination of tar. If carbon dioxide and water are present, syngas may be regenerated at high temperatures. Since Ni/olivine/La$_2$O$_3$/ZrO$_2$ was used as catalyst, it may react with carbon dioxide or water to form additional carbon monoxide and hydrogen as well. Therefore, one can conclude that catalytic reforming of walnut shell with Ni/olivine/La$_2$O$_3$/ZrO$_2$ in a reactor is very effective in transforming tar into hydrogen and CO. El-Rub et al. [22] revealed that tar could be adsorbed on the catalyst active sites and then reformed into CO and H$_2$ by steam and dry gasification processes. According to Guan et al. [23], catalytic reforming reactions can result in the cleavage of the C–C bonds of biomass, thus resulting in a mixture of CO and H$_2$. The interactions involving biomass/Ni/olivine/La$_2$O$_3$/ZrO$_2$ not only increase CO and H$_2$ in the product gas, but they also renew the active surface of Ni/olivine/La$_2$O$_3$/ZrO$_2$ at high temperatures, which informs why more H$_2$ and CO were formed as the temperature increased.

Principally, higher Ni/olivine/La$_2$O$_3$/ZrO$_2$ activity in the biomass may contribute to higher tar conversion and generation of combustible gases. Furthermore, the CH$_4$ yield increased significantly as the temperature increased, thus showing that methanation reactions may increase as a result of the presence of Ni/olivine/La$_2$O$_3$/ZrO$_2$. However, without catalyst addition, the yield of CO$_2$ greatly decreased at higher temperature, as a result of the Boudouard reaction, this is in line with the findings of refs. [1,13,19]. The tar breakdown, water–gas shift reactions and Boudouard reaction all have significant roles in the final CO$_2$ yield. Although the Boudouard reaction and the water–gas shift reaction enhanced CO$_2$ consumption at higher temperatures, tar decomposition reactions may play a large role in CO$_2$ generation under the catalytic performance of Ni/olivine/La$_2$O$_3$/ZrO$_2$; these results are consistent with those of refs. [16,29].

The highest gas yields are majorly those of Hydrogen and carbon(II) oxide at 1100 °C, which are 85H$_2$ yield/mLg^{-1} and 84 yield/mLg^{-1} respectively for biomass/catalyst ratio of 100 g/20 g, while the yields of methane and carbon (IV) oxide were low at 60 yield/mLg^{-1} and 30 yield/mLg^{-1} for biomass/catalyst ratio of 100 g/20 g.

3.7. Effect of steam flow rate on product gas

Fig. 9 shows the variation of product gas composition with steam flowrate in the catalytic reforming of walnut shell. There was an increase
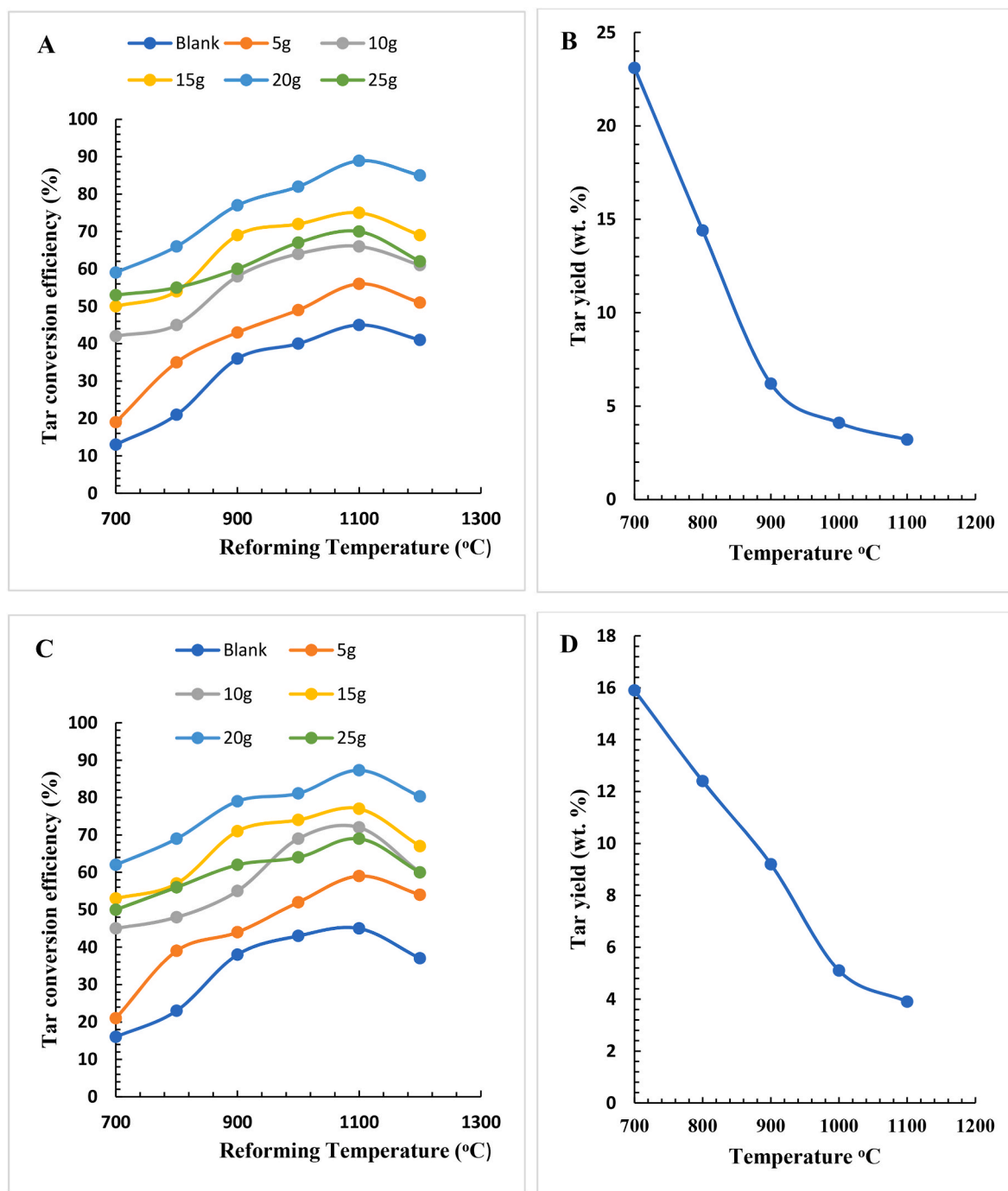
Fig. 7. (a): Effect of reforming temperature on tar conversion at different biomass/catalyst ratio: Condition: Steam flow rate (10 mL/h), (b) Temperature effect on Tar yield wt. %: Condition: Steam flow rate (10 mL/h), (c) Effect of particle size on reforming temperature for tar conversion at different biomass/catalyst ratio: Condition: Particle size (0.2–0.49 mm), (d) Temperature effect on Tar yield wt. %; Condition: Particle size (0.2–0.49 mm).

in the gas concentration of the product gas from 49 mLg^{-1} to 65 mLg^{-1} for hydrogen, 23 mLg^{-1} to 42 mLg^{-1} for CO_2, 14 mLg^{-1} to 24 mLg^{-1} for CO and 11 mLg^{-1} to 13 mLg^{-1} for CH_4 respectively as the steam flow rate rose from 3 mL/h to 9 mL/h. Likewise, the product gas yield (for hydrogen) (Fig. 9), increased from 20.22 mmol/g to 26.02 mmol/g at steam flowrates of 3–9 mL/h; this trend is in line with the results in Refs. [9,17]. The increase in gas yield is as a result of methane steam reforming, water -gas shift as well as steam reforming reactions of tar [24].

The concentration of CO increased from 14 to 24 mLg^{-1} with an increase in steam flow rate, nevertheless, the CO_2 concentration also

increased from 23 mLg^{-1} to 42 mLg^{-1}. The increase in concentrations of CO and CO_2 was most likely due to the water gas-shift reaction, which is exothermic, thus the production of hydrogen is not favorable at high temperatures. Based on Le Chatelier's principle, hydrogen production can be favored when the equilibrium shifts, thus the constraint/concentration on one of the reactants increases, which is induced by the steam flowrate.

At steam flow rate in the range of 2.5–10 mL/h, the H_2/CO ratio increased from 1.93 to 3.06, while the ratio of CO/CO_2 decreased from 2.00 to 1.09 (Table 4) which is an indication of the water gas-shift reaction. Kumagai et al. [25] stated that at 750 °C, there was a rise in the
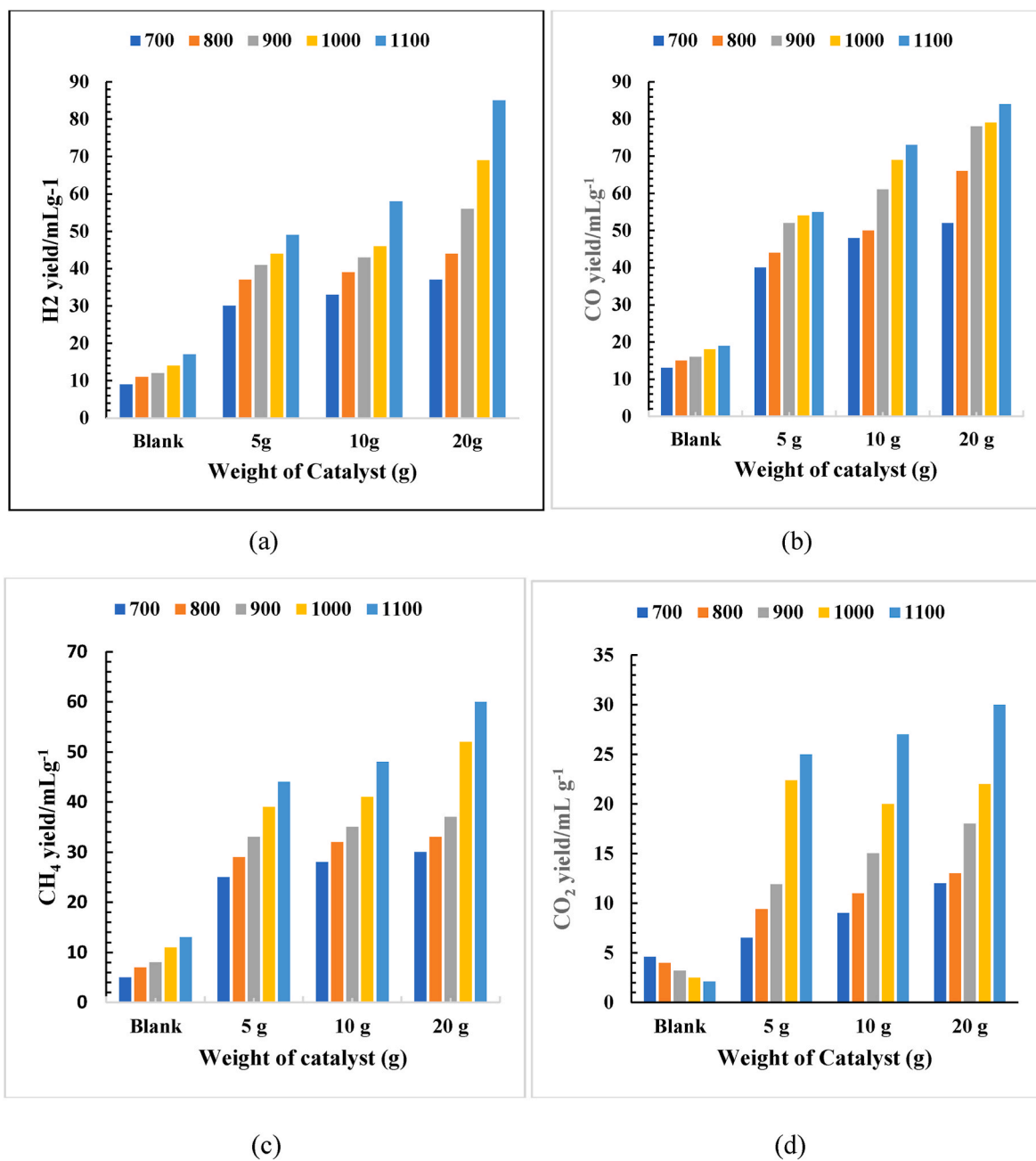
(a)

(b)

(c)

(d)

Fig. 8. Gas composition under different reforming conditions.

concentration of H_2: CO_2 ratio and a reduction in CO: CH_4 ratio during the steam catalytic reforming of rice husk at various SBR from 0.60 to 1.7. The report also shows that hydrogen concentration improved from 48.0 to 52 vol percent with a reduction of carbon(II)oxide concentration from 27.4 to 17.38 mLg^{-1}. The CH_4 concentration slightly increased during the steam reforming process as a result of methanation reaction [18,26]. A reduction in the ratio of hydrogen/methane from 77.34 to 30.11 suggests the formation of methane from methanation reaction. No other hydrocarbons were formed as a result of the high temperature used in this study. Franco et al. [27] analyzed the effect of different SBRs on gas composition and gas yield from wood reforming by gasification at 800 °C in a fluidized bed reactor. The concentration of hydrogen increased when the SBR increased from 0.5 to 0.7. However, when the SBR was further increased, the H_2 concentration decreased. They concluded that at lower SBRs, the steam was very slow to react with the biomass, thus, equilibrium was not attained in the gaseous product, but

at higher SBRs, the water gas shift reaction caused the formation of H_2 and CO_2. Hu et al. [28] also reported similar findings during the reforming of apricot stones at 850 °C, which showed that the yield of hydrogen increased for SBRs of 0.4–0.8 and slightly decreased with further increase in SBRs from 0.8 to 1.2.

3.8. Effect of particle size of walnut shell (biomass) in the catalytic reforming process

Table 5 shows the effect of particle size on walnut shell in the reforming process. The catalyst temperature was fixed at 1000 °C with the steam flow rate maintained at 7.5 mL/h. The biogas yield increased from 49 wt% for particle sizes of 2.5–3.5 mm, to 60.1 wt% for particles of 0.2–0.5 mm. Similar results were obtained in refs, [4,17]. The gas yield increased from 2.18 to 2.42 m^3/kg for 5 mm to <0.15 mm particle size of palm waste biomass and catalytic reforming temperature of
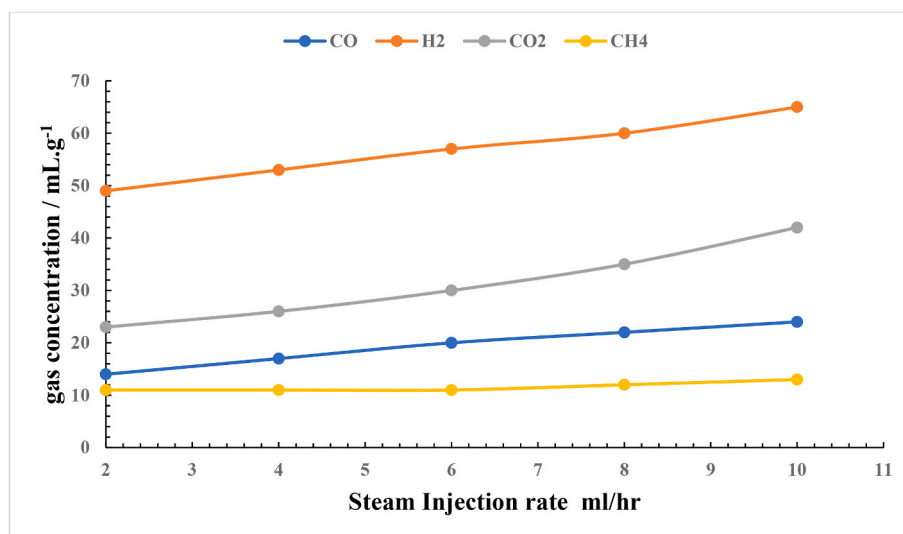
Fig. 9. Effect of steam flow rate on gas composition during biomass reforming at 1000 °C.

Table 4
Effect of steam flowrate on the reforming of the biomass at 1000 °C.

Steam flow rate (mL/h)	2.5	5	7.5	10
SBR	0	1.0	1.5	2.0
H_2(mmol/g walnut shell)	20.22	22.81	24.09	25.99
Hydrogen/Carbon (II) Oxide	1.93	2.12	2.33	3.06
Carbon (II) Oxide/Carbon (IV) Oxide	2.00	1.97	1.26	1.09
Hydrogen/Carbon (IV) Oxide	3.73	4.04	3.22	3.79
Hydrogen/Methane	77.34	39.37	35.48	30.11
Methane/Carbon (II) Oxide	0.04	0.07	0.11	0.14
Methane/Carbon (IV) Oxide	0.03	0.09	0.13	0.16

Table 5
Effects of particle size on catalytic reforming of walnut shell.

Particle size (mm)	0.2–0.49	0.5–0.9	1.5–2.0	2.5–3.5
H_2(mmol/g walnut shell)	29.05	27.09	26.62	24.93
Hydrogen/Carbon (II) Oxide	3.5	2.66	2.47	2.33
Carbon (II) Oxide/Carbon (IV) Oxide	0.91	0.97	1.04	1.27
Hydrogen/Carbon (IV) Oxide	4.01	3.41	3.62	3.81
Hydrogen/Methane	60.18	58.47	50.11	47.05
Methane/Carbon (II) Oxide	0.03	0.05	0.07	0.09
Methane/Carbon (IV) Oxide	0.08	0.10	0.12	0.13

850 °C in a two-stage gasification process carried out at 800 °C by Li et al. [29].

Luo et al. [30] demonstrated that higher gas yield can be as a result of the improved heat and mass transfer from larger surface area to volume ratio and smaller particle diameter imposed by smaller particles which cause most volatiles to evolve, thereby leaving behind highly porous chars. For porous chars, gasification reactions occur not only on the surfaces but also throughout the char; thus, the reaction rate is controlled by chemical kinetics and not mass and heat transfer [19,23]. According to Babu et al. [31], complete conversion of biomass with smaller particle sizes requires lesser time compared to larger particles.

3.9. Effect of particle size on gas composition and the production of hydrogen

The results in Fig. 10 show the concentrations of all product gas where H_2 was slightly improved from 47.05 mL/g (for the 2.5–3.5 mm walnut shells) to 60.18 mL/g (for the 0.2–0.49 mm wall nut shells). Table 5 shows the yield of hydrogen for the catalytic steam reforming

reaction of the biomass. According to Refs. [7,22,27] the concentration of H_2 increased as the particle size decreased owing to the improved gas phase reaction. Wei et al. [32] reported that biomass having particles of smaller sizes tend to release more volatiles. The results of this research show that the variations in biomass particle size exhibited little influence on the production of hydrogen, which may likely have occured as a result of the high temperatures adopted, thus resulting in effective heat transfer within the biomass particles. Furthermore, the properties of the biomass particulates may have been altered in the proximate/ultimate analysis during the process of sieving.

The concentration of CO reduced from 22 to 21 mL/g when the particle size changed from 2.5 - 3.5 mm to 0.2–0.49 mm, thus suggesting hydrogen formation via water gas-shift reaction as shown by an increase in Hydrogen/Carbon (II) Oxide (for the 2.5–3.50 mm particles) with a corresponding decrease in Carbon (II) Oxide/Carbon (IV) Oxide from 1.27 to 0.91 as shown in Table 5.

Conditions: (1000 °C and SBR 1.5).

3.10. Reaction mechanism of the novel catalyst in the catalytic reforming process

Benzene, naphthalene and other aromatic compounds are not generated during the catalytic reforming reaction of tar by Ni/olivine/La_2O_3/ZrO_2, therefore the tar is fully converted into gaseous products after being adsorbed on the active sites of the catalyst. After that the tar has been adsorbed, it then on the catalyst-surface, it then penetrates the pores of the catalyst matrix. Thereafter, reaction then takes place at the interior of the pores to form the desired products, and hence, there is internal diffusion of products through the pores, followed by outer diffusion of the products to the surface of the catalyst which is then completed by the final desorption of gaseous products from the pore-mouth of the catalyst, thus releasing CO_2, H_2, CH_4, and CO [34,35].

Due to the obvious complicated composition of tar, understanding the catalysis and reaction mechanism in the catalyst removal process is difficult. Tar molecules should, in general, be adsorbed on the surface of the catalyst and form intermediates or radicals. Steam as gasifying agent can be adsorbed on the surface of the catalyst with further dissociation into some free radicals (H, OH, and O) which are desorbed alongside the formation of CO_2, CO, H_2, and CH_4 [33]. The diffusion of tar molecules into internal active sites, followed by decomposition and adsorption of tar molecules unto the active sites, are the main processes during catalytic reforming [24]. The pore structure and content of La_2O_3 and ZrO_2 in the catalyst enhances the efficiency of the reforming process. ZrO_2
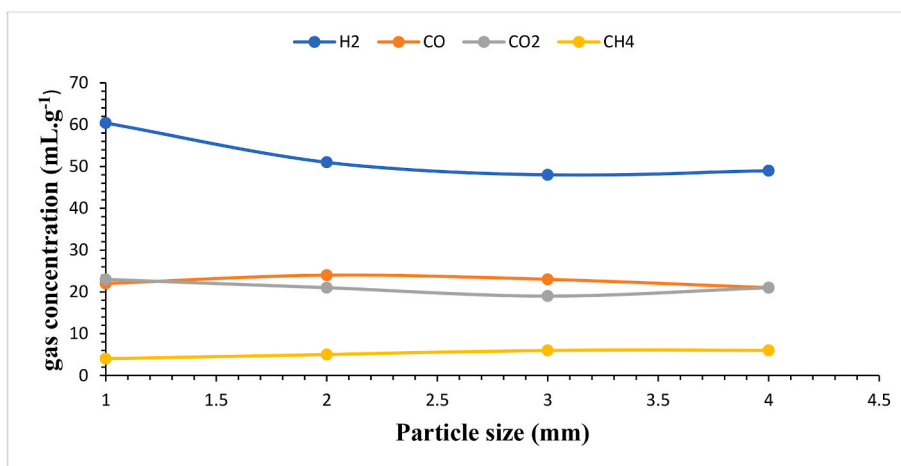
Fig. 10. Concentrations of product gases for different particle sizes of wall nut shells at 1000 °C. **Note: 1 →** (0.2–0.49 mm) **; 2 →** (0.5–0.9 mm)**; 3 →** (1. 5–2.0)**; 4 →** (2.5–3.5 mm)**.

contributed highly accessible specific surface area, good thermal and chemical stabilities during the reforming process, thus improving catalyst-activity; ZrO_2 also provides mechanical stability for the Ni/o-livine/La_2O_3 system.

Through the mesopores and micropores in the catalyst, tar molecules first diffuse into the internal pores of the catalyst. The tar molecules are then adsorbed on the surface of the catalyst and thus dissociate into radicals using La_2O_3 and ZrO_2 as supprts. The radicals' formation is likely the first step in the reaction rate-determining step. The presence of olivine, La_2O_3 and ZrO_2 in the catalyst destabilizes tar molecules, thus rendering them more active and easy to break down into radicals. The degradation of tar molecules is linked to the structure of tar, with variable activation energies for different tar structures. Since they are

relatively active, aromatic compounds containing more penta-cycled rings/substituted groups or fused rings tend to easily breakdown (Fig. 11). Tar dissociated radicals can combine with steam active radicals to produce microscopic tar molecules (CxHy), CO and H_2, thus resulting in the reforming of tar compounds [27]. As the reforming reaction progresses with increase in temperature (Fig. 11), the catalyst promoter and support mechanism will be compromised, thus making the catalyst less active at 1200 °C. At this condition, the rate of formation of radicals is reduced considerably due to insufficient active sites at the later stage of the reforming process, thus resulting in a drop in the performance of the catalyst [31].

Based on related studies, Ni sintering at high temperature, results in loss of catalyst's active surface, pore contraction/closure and
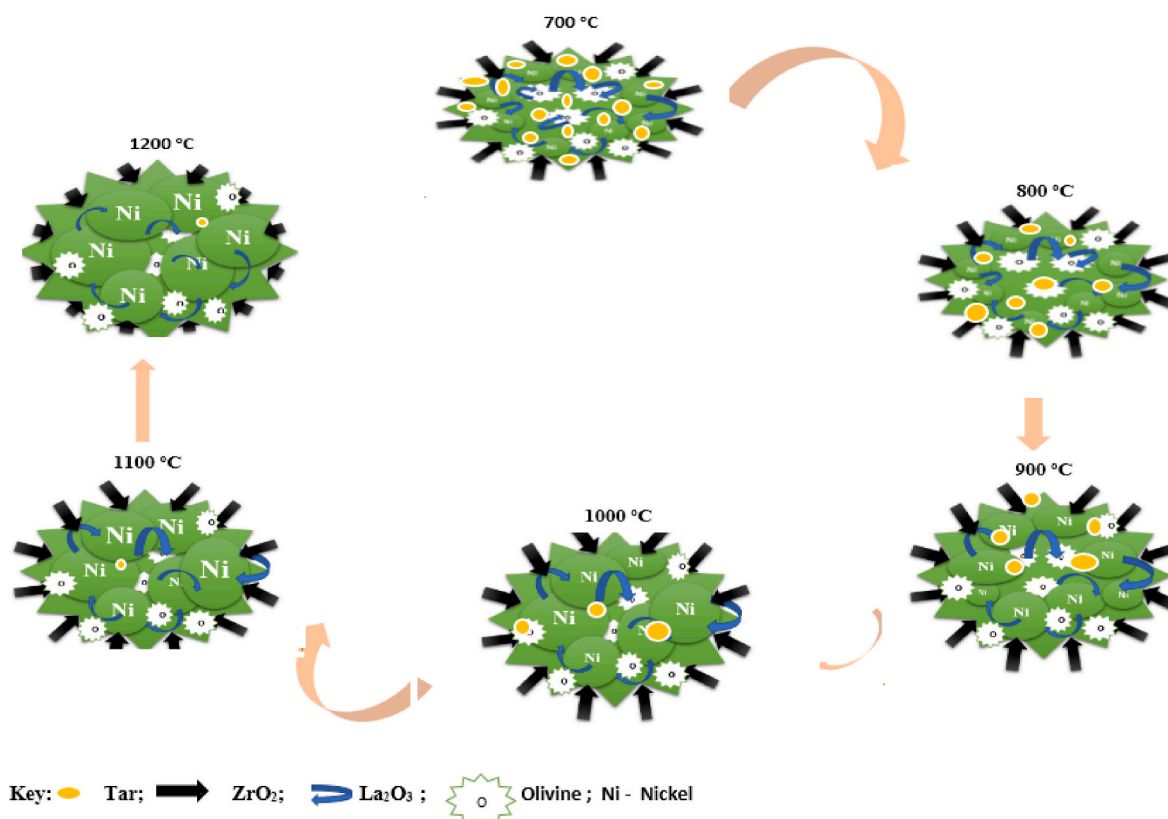

Fig. 11. Mechanism of reaction of tar reforming using Ni/olivine/La_2O_3/ZrO_2.

degradation of catalyst amidst the combined effect of primary encapsulation of metallic nickel due to the collapse of the support structure and sporadic agglomeration of nickel crystallites. Since Ni sintering occurs at high temperature, it then necessitated the inclusion of another catalyst-support i.e., olivine in the $La_2O_3/Ni/ZrO_2$ which helped to prevent Ni-sintering at high temperatures so as to remedy the challenges stated above. Upon increasing the temperature from 700 °C to 1100 °C, with the aid of olivine and La_2O_3, the porosity, average pore size and the permeability of Ni was retained (Fig. 11), which is believed to have helped to stabilize the catalyst thus preventing it from collapsing during the tar reforming process.

3.11. Catalyst regeneration

The structure of the catalyst changes during tar removal, thus affecting the porous structure, active sites, and surface area of the catalyst. These factors can cause the catalyst's activity to drop and perhaps deactivate. The operating conditions in tar catalytic reforming, such as complex reaction atmosphere, high reaction temperature, and longer residence time, are all factors that influenced the performance of the catalyst in these modifications. When the catalyst's activity drops to a crucial limit, it then becomes necessary to regenerate the catalyst.

The catalyst's long-term catalytic activity was further investigated at 500 °C with in situ regeneration in 15 vol percent O_2 in roughly 12 vol percent steam for 0.5 h at 600 °C. During catalytic regeneration, traces of (tars) aromatics were identified in the product gas, but no CO_2 or CO was identified. The catalyst was fully functional once more, and no trace of tar was discovered using the GC. The catalyst did not completely deactivate, although it was only active for a limited time after the final regeneration (1 h). The catalyst functioned for 96 h during that time, thus requiring four regeneration cycles. Also, during the first three regeneration cycles involving the use of oxygen, a temperature increase at the catalyst inlet was observed.

4. Conclusion

The catalytic performance/reforming effect of $Ni/olivine/La_2O_3/ZrO_2$ on walnut shell biomass was studied. $Ni/olivine/La_2O_3/ZrO_2$ exhibited good characteristics with highly porous structure as well as improved catalytic and tar reforming of volatiles from biomass (walnut shell) to produce syngas. The improved hydrogen production was as a result of the water gas-shift reaction towards enhancing hydrogen production via CO_2 absorption on the catalyst site during the reforming process. Temperature has an important effect on the product gases produced during tar reforming. Under the conditions of rapid heating rates, larger amounts of gases were produced. Biomass-derived volatiles and tar were found to accumulate on the catalysts surface, thus promoting high catalytic activity. As a result, when the regenerated catalysts were employed, more gas was produced. From the results obtained, $Ni/olivine/La_2O_3/ZrO_2$ gave higher tar conversion efficiency of the walnut shell biomass. The tar conversion efficiencies of the walnut shell biomass are 98.9%, 92.0% and 89.4%, respectively for the 20, 15 and 5 g $Ni/olivine/La_2O_3/ZrO_2$ catalysts respectively. An increase in temperature favored higher gas yield. The smallest particle size gave the highest H_2 yield whereas, this was not so for other gases as increased particle size gave random variations in the gas yields of CH_4, CO and CO_2. Furthermore, at low flow rates of say, 2.5 L/h, the H_2/CH_4 ratio was highest (77.4) which is indicative of more hydrogen production, however at higher flow rates, more methane was formed relative to H_2; the results are thus suggestive of the tendency to tweak the reaction in favor of the gas of interest i.e., whether hydrogen or methane. The optimal quantity of catalyst that gave the highest tar conversion is 20 g, hence, it is advisable to adopt the specified catalyst weight for high tar-reformation to syngas.

Declaration of competing interest

The authors declare that they have no known competing financial interests or personal relationships that could have appeared to influence the work reported in this paper.

Appendix A. Supplementary data

Supplementary data to this article can be found online at https://doi.org/10.1016/j.joei.2022.05.004.

References

[1] L. Santamaria, A. Arregia, G. Lopeza, M. Artetxe, M. Amutio, M. Olazara, Effect of La2O3 promotion on a Ni/Al2O3 catalyst for H2 production in the inline biomass pyrolysis-reforming, Fuel 262 (2020), 116593.

[2] B.L. Dou, H. Zhang, Y.C. Song, L.F. Zhao, B. Jiang, M.X. He, C.J. Ruan, H.S. Chen, Y.J. Xu, Hydrogen production from the thermochemical conversion of biomass: issues and challenges, Sustain, Energy Fuels 3 (2019) 314–342, https://doi.org/10.1039/c8se00535d.

[3] C.T. Zhang, L.J. Zhang, Q.Y. Li, Y. Wang, Q. Liu, T. Wei, D.H. Dong, S. Salavati, M. Gholizadeh, X. Hu, Catalytic pyrolysis of poplar wood over transition metal oxides: correlation of catalytic behaviors with physiochemical properties of the oxides, Biomass Bioenergy 124 (2019) 125–141, https://doi.org/10.1016/j.biombioe.2019.03.017.

[4] F.Q. Guo, X.M. Zhao, K.Y. Peng, S. Liang, X.P. Jia, L. Qian, Catalytic reforming of biomass primary tar from pyrolysis over waste steel slag-based catalysts, Int. J. Hydrogen Energy 44 (2019) 16224–16233, https://doi.org/10.1016/j.ijhydene.2019.04.190.

[5] P. Knutsson, V. Cantatore, M. Seemann, P.L. Tam, I. Panas, Role of potassium in the enhancement of the catalytic activity of calcium oxide towards tar reduction, Appl. Catal. B Environ. 229 (2018) 88–95, https://doi.org/10.1016/j.apcatb.2018.02.002.

[6] R.S. Tan, T.A.T. Abdullah, S.A. Mahmud, R.M. Zin, K.M. Isa, Catalytic steam reforming of complex gasified biomass tar model toward hydrogen over dolomite promoted nickel catalysts, Int. J. Hydrogen Energy 44 (2019) 21303–21314, https://doi.org/10.1016/j.ijhydene.2019.06.125.

[7] Z. Xi, U. Yasuaki, Y. Ryo, N. Ichiro, W. Fang, H. Zhennan, X. Guangwen, Recent progress in tar removal by char and the applications: a comprehensive analysis, Carbon Resour. Convers. (2019), https://doi.org/10.1016/j.crcon.2019.12.001. S258891331930050X.

[8] T. Higo, H. Saito, S. Ogo, Y. Sugiura, Y. Sekine, Promotive effect of Ba addition on the catalytic performance of Ni/LaAlO3 catalysts for steam reforming of toluene, Appl. Catal. A-Gen. 530 (2017) 125–131, https://doi.org/10.1016/j.apcata.2016.11.026.

[9] Z.H. Min, P. Yimsiri, M. Asadullah, S. Zhang, C.Z. Li, Catalytic reforming of tar during gasification. Part II. Char as a catalyst or as a catalyst support for tar reforming, Fuel 90 (7) (2011) 2545–2552.

[10] S. Zhang, M. Asadullah, L. Dong, H.L. Tay, C.Z. Li, An advanced biomass gasification technology with integrated catalytic hot gas cleaning. Part II: tar reforming using char as a catalyst or as a catalyst support, Fuel 112 (2013) 646–653.

[11] V. Balasundram, K.K. Zaman, N. Ibrahim, R.M. Kasmani, R. Isha, M.K.A. Hamid, H. Hasbullah, Catalytic upgrading of pyrolysis vapours over metal modified HZSM-5 via in-situ pyrolysis of sugarcane bagasse: effect of nickel to cerium ratio on HZSM-5, J. Anal. Appl. Pyrolysis 134 (2018) 309–325, https://doi.org/10.1016/j.jaap.2018.06.021.

[12] J.A. Rached, M.R. Cesario, J. Estephane, H.L. Tidahy, C. Gennequin, S. Aouad, A. Aboukais, E. Abi-Aad, Effects of cerium and lanthanum on Ni-based catalysts for CO2 reforming of toluene, J. Environ. Chem. Eng. 6 (2018) 4743–4754, https://doi.org/10.1016/j.jece.2018.06.054.

[13] L. Santamaria, G. Lopez, A. Arregi, M. Amutio, M. Artetxe, J. Bilbao, M. Olazar, Effect of calcination conditions on the performance of Ni/MgO-Al2O3 catalysts in the steam reforming of biomass fast pyrolysis volatiles, Catal. Sci. Technol. 9 (2019) 3947–3963, https://doi.org/10.1039/c9cy00597h.

[14] L. Santamaria, A. Arregi, J. Alvarez, M. Artetxe, M. Amutio, G. Lopez, J. Bilbao, M. Olazar, Performance of a Ni/ZrO2 catalyst in the steam reforming of the volatiles derived from biomass pyrolysis, J. Anal. Appl. Pyrolysis 136 (2018) 222–231, https://doi.org/10.1016/j.jaap.2018.09.025.

[15] E. Savuto, R.M. Navarro, N. Mota, A. Di Carlo, E. Bocci, M. Carlini, J.L.G. Fierro, Steam reforming of tar model compounds over Ni/Mayenite catalysts: effect of Ce addition, Fuel 224 (2018) 676–686, https://doi.org/10.1016/j.fuel.2018.03.081.

[16] F. Yang, J. Cao, X. Zhao, J. Ren, W. Tang, X. Huang, X. Feng, M. Zhao, X. Cui, X. Wei, Acid washed lignite char supported bimetallic Ni-Co catalyst for low temperature catalytic reforming of corncob derived volatiles, Energy Convers. Manag. 196 (2019) 1257–1266, https://doi.org/10.1016/j.enconman.2019.06.075.

[17] 4 more authors M. Ye, Y. Tao, F. Jin, et al., Enhancing hydrogen production from the pyrolysis-gasification of biomass by size-confined Ni catalysts on acidic MCM-41 supports, Catal. Today 307 (2018) 154–161, https://doi.org/10.1016/j.cattod.2017.05.077. ISSN 0920-5861.

[18] P. Daorattanachai, W. Laosiripojana, A. Laobuthee, N. Laosiripojana, Type of contribution: research article catalytic activity of sewage sludge char supported Re-Ni bimetallic catalyst toward cracking/reforming of biomass tar, Renew. Energy 121 (2018) 644–651, https://doi.org/10.1016/j.renene.2018.01.096.

[19] M. Hu, M. Laghari, B.H. Cui, B. Xiao, B.P. Zhang, D.B. Guo, Catalytic cracking of biomass tar over char supported nickel catalyst, Energy 145 (2018) 228–237, https://doi.org/10.1016/j.energy.2017.12.096.

[20] H.Y. Xu, Y.N. Liu, G.W. Sun, S.F. Kang, Y.G. Wang, Z. Zheng, X. Li, Synthesis of graphitic mesoporous carbon supported Ce-doped nickel catalyst for steam reforming of toluene, Mater. Lett. 244 (2019) 123–125, https://doi.org/10.1016/j.matlet.2019.02.058.

[21] X.B. Wang, S.Q. Yang, C. Xu, H.D. Ma, Z.H. Zhang, Z.Y. Du, W.Y. Li, Effect of boron doping on the performance of Ni/Biochar catalysts for steam reforming of toluene as a tar model compound, J. Anal. Appl. Pyrolysis 155 (2021), https://doi.org/10.1016/j.jaap.2021.105033.

[22] A. Z El-Rub, E.A. Bramer, G. Brem, Review of catalysts for tar elimination in biomass gasification processes, Ind. Eng. Chem. Res. 43 (2004) 6911–6919.

[23] G.Q. Guan, M. Kaewpanha, X.G. Hao, A. Abudula, Catalytic steam reforming of biomass tar: prospects and challenges, Renew. Sustain. Energy Rev. 58 (2016) 450–461.

[24] B.A. Oni, S. E Sanni, P.M. O Ikhazuangbe, A.J. Anayo, Experimental investigation of steam-air gasification of Cymbopogon citratus using Ni/dolomite/CeO2/K2CO3 as catalyst in a dual stage reactor for syngas and hydrogen production, Energy 237 (2021), 121542.

[25] S. Kumagai, J. Alvarez, P.H. Blanco, C. Wu, T. Yoshioka, M. Olazar, P.T. Williams, Novel Ni-Mg-Al-Ca catalyst for enhanced hydrogen production for the pyrolysis/gasification of a biomass/plastic mixture, J. Anal. Appl. Pyrolysis 113 (2015) 15–21.

[26] A. K Olaleye, K. J Adedayo, C. Wu, M.A. Nahil, M. Wang, P.T. Williams, Experimental study, dynamic modelling, validation and analysis of hydrogen production from biomass pyrolysis/gasification of biomass in a two-stage fixed bed reaction system, Fuel 137 (2014) 364–374, https://doi.org/10.1016/j.fuel.2014.07.076.

[27] C. Franco, F. Pinto, I. Gulyurtlu, I. Cabrita, The study of reactions influencing the biomass steam gasification process, Fuel 82 (2003) 835–842.

[28] S. Hu, J. Xiang, L.S. Sun, M.H. Xu, J.R. Qiu, P. Fu, Characterization of char from rapid pyrolysis of rice husk, Fuel Process. Technol. 89 (11) (2008) 1096–1105.

[29] L. Li, K. Morishita, H. Mogi, K. Yamasaki, T. Takarada, Low-temperature gasification of a woody biomass under a nickel-loaded brown coal char, Fuel Process. Technol. 91 (2010) 889–894.

[30] S. Luo, B. Xiao, X. Guo, Z. Hu, S. Liu, M. He, Hydrogen-rich gas from catalytic steam gasification of biomass in a fixed bed reactor: influence of particle size on gasification performance, Int. J. Hydrogen Energy 34 (2009) 1260–1264.

[31] H. Yu, J. Liu, H. Yang, Catalytic reforming of volatiles from pyrolysis of biomass components over a novel Ni/magnesium slag catalyst, J. Anal. Appl. Pyrol. 159 (2021), 105316.

[32] L. Wei, S. Xu, L. Zhang, H. Zhang, C. Liu, H. Zhu, S. Liu, Characteristics of fast pyrolysis of biomass in a free fall reactor, Fuel Process. Technol. 87 (2006) 863–871.

[33] Xiao-Yan Zhao, Jie Ren, Jing-Pei Cao, Fu Wei, Chen Zhu, Xing Fan, Yun-Peng Zhao, Xian-Yong Wei, Catalytic reforming of volatiles from biomass pyrolysis for hydrogen-rich gas production over limonite ore, Energy Fuel. 31 (4) (2017) 4054–4060, https://doi.org/10.1021/acs.energyfuels.7b00005.

[34] Z. Min, P. Yimsiri, M. Asadullah, S. Zhang, C. Li, Catalytic reforming of tar during gasification. Part II, in: Char as a catalyst or as a catalyst support for tar reforming 90, 2011, pp. 2545–2552, https://doi.org/10.1016/j.fuel.2011.03.027, 7.

[35] Y. Liu, M. Paskevicius, H. Wang, G. Parkinson, J. Wei, M.A. Akhtar, C. Li, Insights into the mechanism of tar reforming using biochar as a catalyst, Fuel 296 (120672) (2021).